Single Ion as a Three-Body Reaction Center in an Ultracold Atomic Gas

Arne Härter, Artjom Krükow, Andreas Brunner, Wolfgang Schnitzler, Stefan Schmid, and Johannes Hecker Denschlag

Institut für Quantenmaterie and Center for Integrated Quantum Science and Technology IQST, Universität Ulm, 89069 Ulm, Germany

(Received 1 June 2012; published 18 September 2012)

We report on three-body recombination of a single trapped Rb^+ ion and two neutral Rb atoms in an ultracold atom cloud. We observe that the corresponding rate coefficient K_3 depends on collision energy and is about a factor of 1000 larger than for three colliding neutral Rb atoms. In the three-body recombination process large energies up to several 0.1 eV are released leading to an ejection of the ion from the atom cloud. It is sympathetically recooled back into the cloud via elastic binary collisions with cold atoms. Further, we find that the final ionic product of the three-body processes is again an atomic Rb^+ ion suggesting that the ion merely acts as a catalyzer, possibly in the formation of deeply bound Rb_2 molecules.

DOI: 10.1103/PhysRevLett.109.123201 PACS numbers: 34.50.Lf, 37.10.Rs

Early on in the quest for ultracold quantum gases, three-body recombination played a crucial role as a limiting factor for Bose-Einstein condensation. It was first investigated in spin-polarized hydrogen [1] and somewhat later for alkali atoms [2,3]. Recently, three-body recombination was investigated with single atom resolution [4]. Combining ultracold atoms with cold trapped ions is an emerging field where large scattering cross sections naturally come into play due to the comparatively long range $1/r^4$ polarization interaction potential. Two-body collisions between atoms and ions in the low energy regime have been recently studied [5–11]. In this Letter, we report on three-body collisions involving two ultracold ^{87}Rb atoms and a $^{87}Rb^+$ ion at mK temperatures. The ion in our experiment can be regarded as a reaction center, facilitating molecule formation through its large interaction radius.

For the work presented here, it is essential that we work with ions and atoms of the same species. This renders charge transfer reactions irrelevant, which otherwise would strongly constrain our measurements. As Rb^+ is not amenable to laser cooling and cannot be imaged, we detect the ion and investigate its dynamics in an indirect way, i.e., through its action on the atom cloud. In our experiments, we place a single ion into the center of an atomic sample resulting in a continuous loss of atoms due to elastic atom-ion collisions. This behavior is interrupted when a highly energetic three-body process ejects the ion from the atom cloud. By examining the statistics of ion-induced atom loss in hundreds of repetitions of the experiment, we can investigate a number of important details of the three-body process, such as its quadratic density dependence, the energy that it releases, its rate coefficient K_3, the dependence of K_3 on collisional energy, and its reaction products. Furthermore, our measurements also demonstrate sympathetic cooling of an ion from eV energies down to about 1 mK using an ultracold buffer gas.

The atom-ion collision experiments are conducted in a hybrid apparatus (for details see Ref. [12]) where a single $^{87}Rb^+$ ion, trapped in a linear Paul trap, is brought in contact with an ultracold cloud of spin polarized ^{87}Rb atoms ($F = 1$, $m_F = -1$). The atom cloud is previously prepared at a separate location from where it is transported to the Paul trap and loaded into a far off-resonant crossed optical dipole trap. The dipole trap is at first spatially separated from the trapped ion by about 50 μm. To start the atom-ion collision experiments, it is then centered on the ion with μm precision within a few 100 ms. At this point the atom cloud consists of $N_{at} \approx 4.0 \times 10^4$ atoms at a temperature of $T_{at} \approx 1.2$ μK and a peak density $n_{at} \approx 1.1 \times 10^{12}$ cm^{-3}. At trapping frequencies of (190, 198, 55) Hz this results in a cigar shaped cloud with radial and axial extensions of about 10 and 35 μm, respectively.

The single Rb^+ ion is confined in a Paul trap driven at a frequency of 4.17 MHz resulting in radial and axial trapping frequencies of 350 and 72 kHz, respectively. As the trap is about 4 eV deep, the ion typically remains trapped for thousands of experimental cycles. It is initially produced by photoionization of an atom from a cold Rb cloud in the Paul trap [13]. Typical kinetic energies E_{ion} of the ion after sympathetic cooling in the atom cloud are about a few mK $\cdot$ k_B. This energy scale is mainly set by two quantities: (1) The excess micromotion [14] in the Paul trap whose main part we can control by compensating stray electric fields [13]. (2) Heating effects induced by the interplay of micromotion and elastic collisions [15–17].

As described in Ref. [8], an ion immersed in an ultracold atom cloud leads to atom loss by expelling atoms from the shallow optical trap (≈ 10 μK $\cdot$ k_B trap depth) via elastic collisions. The radio frequency (rf) driven micromotion is a constant source of energy which drives these loss-afflicting collisions. Figure 1(a) shows such a decay of an atom cloud at relatively low densities ($\approx 10^{11}$ cm^{-3}) and

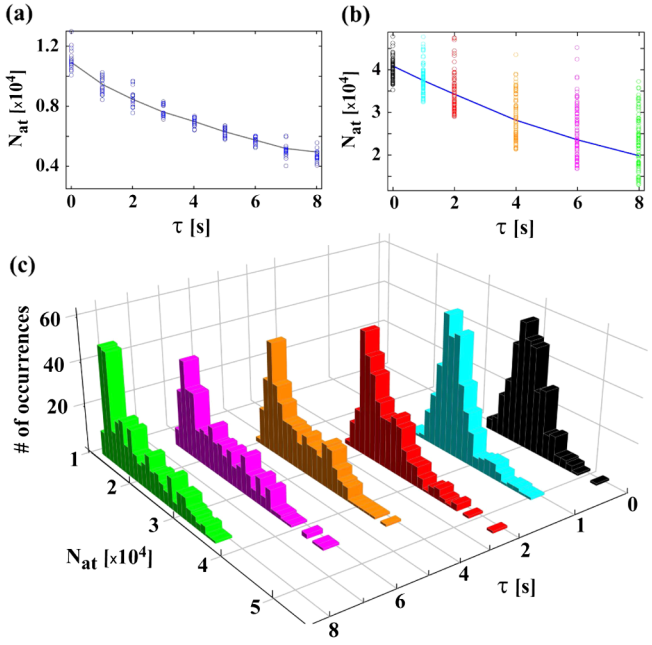

FIG. 1 (color online). Decay of the atom cloud under influence of a single trapped ion. (a) Remaining atom numbers after interaction time τ for an ion with $E_{\text{ion}} \approx 35\ \text{mK} \cdot k_B$ [18] and $n_{at} \approx 10^{11}\ \text{cm}^{-3}$. The solid line indicates the decay of the mean atom number. (b) Same as (a) but $E_{\text{ion}} \approx 0.5\ \text{mK} \cdot k_B$ [18] and $n_{at} \approx 1.1 \times 10^{12}\ \text{cm}^{-3}$. (c) Histograms containing the data shown in (b).

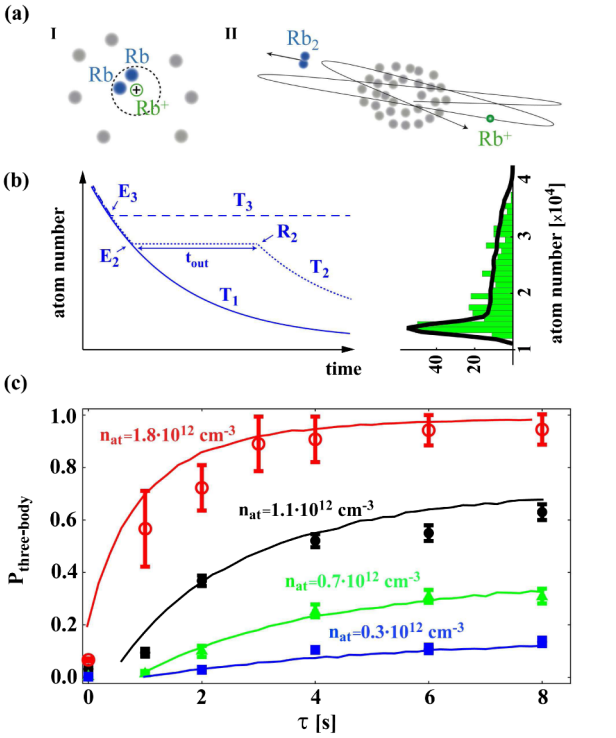

FIG. 2 (color online). (a) Illustration of an atom-atom-ion collision. (I) Two atoms simultaneously enter the interaction radius of the ion and a three-body process takes place. (II) The three-body reaction ejects the ion onto a trajectory much larger than the atom cloud. (b) Illustration of our simple model. *Left:* Various possible time traces for the atom number. If only binary atom-ion collisions occur the atomic sample decays exponentially (Trace T_1). Three-body events (E_2, E_3) interrupt the atom loss until the atom is recooled and reenters the sample at point R_2 (Traces T_2 and T_3). *Right:* Atom number histogram from Fig. 1(c) ($\tau = 8$ s) and the corresponding simulation result (solid black line). (c) Plot of the probability $P_{\text{three-body}}$ for initial atomic densities $(1.8, 1.1, 0.7, 0.3) \times 10^{12}\ \text{cm}^{-3}$ and atom numbers $(6.5, 4.0, 2.8, 1.6) \times 10^4$, respectively. The solid lines are results of the numerical simulation.

relatively high ion energies ($\approx 35\ \text{mK} \cdot k_B$ [18]). Plotted is the number of remaining atoms after an atom-ion interaction time τ. Each data point corresponds to a single measurement. Overall, the plot shows a relatively smooth decay of the atom cloud with a relative scatter of the atom number of less than 10%. This changes drastically when we carry out the experiments at low ion energies ($\approx 0.5\ \text{mK} \cdot k_B$ [18]) and larger densities ($\approx 10^{12}\ \text{cm}^{-3}$) [Fig. 1(b)]. Here, the scatter dramatically increases with τ and is on the order of the number of lost atoms. In Fig. 1(c) histograms are shown which contain the data of Fig. 1(b). With increasing time τ, the initial Gaussian distribution develops a striking tail towards large atom numbers. At the tips of the tails we find cases where even after interaction times of several seconds barely any atoms have been lost, a signature of missing atom-ion interaction. Apparently, sporadically the ion is ejected from the atom cloud and promoted onto a large orbit for a period of time during which atom-ion collisions are negligible [Fig. 2(a)]. In principle, this is reminiscent of the energy distributions with high energy tails that have recently been predicted for trapped ions immersed in a buffer gas [15,16]. However, it turns out that such an explanation is inconsistent with our observations on the grounds of energetics and scaling. Rather, we find that it is a three-body recombination process involving the ion and two neutrals that ejects the ion from the cloud. Due to the large trap depth the ion is not lost in such an event, but it is recooled back into the cloud through binary collisions after some time.

Figure 2(b) illustrates in a simple picture how the decay of the atom number over time can follow different paths. The solid trace T_1 shows the case when only binary atom-ion collisions occur. Such traces result in the narrow Gaussian peak of the atom number distribution shown on the right of Fig. 2(b). Traces T_2 and T_3 exhibit three-body collisions at points E_2 and E_3. At point R_2 the ion reenters the atom cloud after an interruption time t_{out}. Rare three-body events and long times t_{out} result in a long tail of the distribution. We can reproduce the histograms in Fig. 1 with a simple Monte Carlo type simulation (for details see Supplemental Material [19]). We assume an initial Gaussian distribution of the atom number which then decays exponentially with the binary atom-ion collision rate $K_2 n_{at}$. Here, K_2 is a rate constant given by the product

of the elastic cross section and the ion velocity. A three-body event, occurring at a rate $K_3 n_{at}^2$, interrupts this decay for a period t_{out}. As the ion can only be recooled by the atomic sample, we assume the rate for reentry of the ion into the atom cloud to be proportional to the number of atoms $1/\langle t_{out}\rangle = N_{at}/c_{out}$ with c_{out} being a constant that depends on the trap parameters. Figure 2(b) (right) shows exemplarily that the model can describe well the histograms in Fig. 1. In the following, we continue the analysis by studying $P_{\text{three-body}}$ which is the probability that at least one three-body process takes place within time τ. For each τ we determine $P_{\text{three-body}}$ from our histograms. $P_{\text{three-body}}$ is the count number of the tail of a histogram divided by the histogram's total count number (for details see Supplemental Material [19]). Figure 2(c) shows these data for four atomic densities, including the data in Fig. 1(c). All four data sets have in common that the number of three-body events first rapidly increases and subsequently levels off. The levelling off is mainly due to the fact that the probability for a three-body reaction is strongly density-dependent. Surprisingly, in the beginning of the interaction ($\tau \lesssim 1$ s) only very few three-body events are detected for the lower density samples. We explain this delay by an initial phase of sympathetic cooling of the Rb^+ ion which experiences significant heating during the preparation (e.g., rf evaporative cooling) of the atom cloud. From numerical calculations similar to Ref. [16] we estimate that recooling times of about 1 s in atom clouds with $n_{at} \approx 10^{12}$ cm^{-3} correspond roughly to ion kinetic energies of a few 100 K $\cdot\, k_B$. The ion will typically undergo several thousand binary collisions with cold atoms until it is sympathetically recooled to mK $\cdot\, k_B$ energies. We are able to describe all four data sets in Fig. 2(c) consistently with our simple Monte Carlo model (continuous lines) [20]. From a fit to the data sets we obtain rate coefficients $K_2 = 5.0(5) \times 10^{-9}$ cm^3/s and $K_3 = 3.3(3) \times 10^{-25}$ cm^6/s and the reentry parameter $c_{out} \approx 1.7 \times 10^5$ s. The errors given exclude systematic uncertainties in the atomic density. We note that the value for our atom-atom-ion K_3 rate coefficient is more than three orders of magnitude larger than the three-body coefficient for three colliding neutral ^{87}Rb atoms [2]. The value of K_2 roughly agrees with previously obtained results [7,8]. For the typical atom numbers used here the obtained value of c_{out} results in several seconds of negligible atom-ion interaction following each ejection of the ion.

In order to challenge our analysis we have attempted to model the events that send the ion into orbit as two-body processes. The corresponding linear density dependence of the event rate yields inconsistent fit results such that we can exclude two-body interactions as an explanation for our data (for details see Supplemental Material [19]). As a cautionary note, we point out that three-body recombination processes to weakly bound molecular states with binding energies $\lesssim 10$ meV are not detected in our experiments as the ion will not leave the atom cloud. Thus, the true three-body coefficient may even be significantly larger.

In a further experiment, we quantify the kinetic energy gained by the ion in a three-body event. The idea is to lower the depth of the ion trap such that an ion with an energy of a few 0.1 eV escapes while a cold ion remains trapped. The experiment is performed as follows. We prepare a first atom cloud which we bring to interaction with an ion for 4 s. Similar to the previously described experiments, we measure the ion-induced atom loss from which we judge whether or not the ion has participated in a three-body event. Directly afterwards, the ion trap depth is reduced to one of 5 values U_{red} by lowering one of the end cap voltages of the Paul trap within 300 ms. The voltage is held at this value for 200 ms and ramped back up within 200 ms. Subsequently, we probe the ion's presence in the trap via the loss it inflicts on a second atom cloud. This cloud is prepared within 40 s and contains about 5×10^4 atoms. Figure 3(a) shows the remaining atom number of the atom cloud after 6 s of interaction time [21]. An atom number $\lesssim 1 \times 10^4$ indicates the presence of an ion while a number around 4.5×10^4 shows its absence. The clear splitting of the two groups of data allows for ion detection with an efficiency close to unity. Figure 3(a) contains two different plot symbols, distinguishing two classes of ions. Black squares correspond to ions that have participated in a three-body event within the first atom cloud while grey circles correspond to ions where only binary collisions were detected. We now analyze the data points of

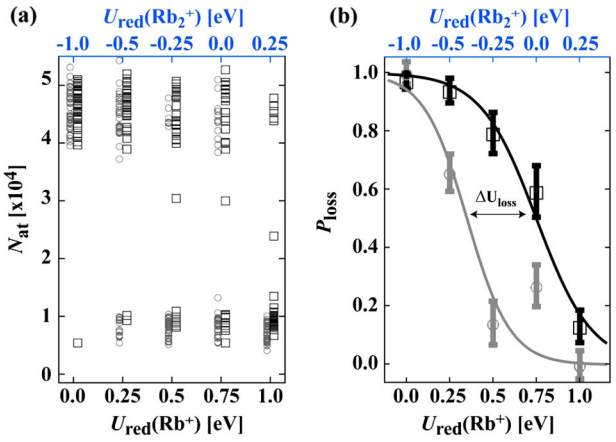

FIG. 3 (color online). (a) Probing the ion's presence using an atom cloud. A low (high) remaining atom number N_{at} signals the presence (absence) of an ion. For better visibility, we have slightly offset in energy the black squares corresponding to ions that have participated in a three-body process from the grey circles corresponding to ions where purely binary collisions were detected. (b) Ion loss probability P_{loss} calculated from the data in (a). The continuous lines are fits to the data using a broadened step function. The trap depths U_{red} are determined for our Paul trap geometry using methods detailed in Ref. [22] for both Rb^+ (bottom abscissa scale) and Rb_2^+ (top). A trap with negative trap depth value is nontrapping.

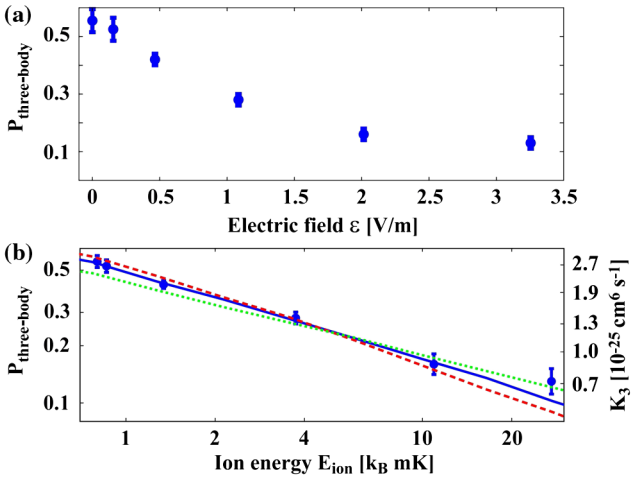

FIG. 4 (color online). (a) $P_{\text{three-body}}$ as a function of the external electric field. (b) Double-logarithmic plot of $P_{\text{three-body}}$ as a function of the ion energy E_{ion} [18]. A scale for the three-body coefficients K_3 as derived from the simulation is also given (see text for details).

Fig. 3(a) by calculating the probability for ion loss P_{loss} for each trap depth (P_{loss} = Number of lost ions/Number of trials). The result is shown in Fig. 3(b). As expected, ions that were previously involved in a three-body recombination process can in general escape from deeper traps than ions only involved in binary interactions. To obtain a more quantitative measure of the ion energy we fit broadened step functions of the form $1/[1 + \exp\{(U_{\text{red}} - U_{\text{loss}})/d\}]$ to the data. The width of the steps d is on the order of 0.15 eV. From the energy offset between the two fit curves we estimate the gained energy $\Delta U_{\text{loss}} \approx 0.4$ eV. We note that for trap depths $U_{\text{red}} \lesssim 0.25$ eV the probability of loss is high in general. This suggests that the stability of our trap is compromised at shallow trap settings. In fact, lowering the voltage of only one of the two end caps renders the trap quite asymmetric. This degrades the ideal quadrupole field configuration and thus the stability of the ion trap. As a consequence, the accuracy with which we can determine the energy released in the three-body process is limited. Still, we find a clear splitting between the step functions of 0.4 eV in Fig. 3(b). Thus, a resolution of the measurement on the order of 0.1 eV seems plausible.

Mainly two recombination processes come into consideration. In a reaction of the type $\text{Rb} + \text{Rb} + \text{Rb}^+ \rightarrow \text{Rb}_2 + \text{Rb}^+$ the formation of a neutral molecule is catalyzed by the ion which carries away 2/3 of the energy released. If deeply bound Rb_2 molecules are produced, binding energies of up to $\sim$0.5 eV are released, in agreement with the measurement. A second possible recombination process, $\text{Rb} + \text{Rb} + \text{Rb}^+ \rightarrow \text{Rb}_2^+ + \text{Rb}$, produces a molecular ion and a neutral atom. However, as indicated in Fig. 3, the molecular ion, due to its higher mass, experiences a significantly shallower trap than the atomic ion and would immediately be lost for our parameter range. We thus infer that the ion at hand is Rb^+. However, we cannot completely exclude the formation of an intermediate molecular ionic state which may subsequently dissociate.

In a third type of measurement, we study the dependence of the three-body coefficient on the ion kinetic energy which we can tune by controlling the ion micromotion. For this we apply a static electric field ε perpendicular to the axis of the Paul trap and let the ion interact for $\tau = 8$ s with an atom cloud with $n_{\text{at}} \approx 1.0 \times 10^{12}$ cm^{-3}. We find $P_{\text{three-body}}$ to increase roughly by a factor of 5 when reducing ϵ from 3.25 V/m to 0 V/m [Fig. 4(a)].

In order to express the electric field values in terms of kinetic energy, we make use of the relation $E_{\text{EMM}} = c_{\text{trap}}\epsilon^2 + E_{\text{res}}$ with c_{trap} being a constant that depends on the trap configuration and the ion mass [14]. E_{res} stands for residual uncompensated micromotion energy. The ion energy can be expressed as $E_{\text{ion}} = c_{\text{dyn}}E_{\text{EMM}}$ [18]. c_{dyn} is a constant which depends on the atom-ion mass ratio and the spatial extension of the atom cloud and for our experiments can be estimated to be about 2 [16]. We attempt to describe our data with a power-law dependence of the form $K_3 \propto E_{\text{ion}}^{\alpha}$ within our simulation. Good agreement with the data is achieved for $\alpha = -0.43$, $E_{\text{res}} = 370\ \mu\text{K} \cdot k_{\text{B}}$ and a maximal value for K_3 of 2.75×10^{-25} cm^6/s [solid trace in Fig. 4(b)]. For comparison, curves for exponents $\alpha = -0.5$ and $\alpha = -0.33$ (dashed and dotted traces, respectively) are shown as well. A residual energy $E_{\text{res}} = 370\ \mu\text{K} \cdot k_{\text{B}}$ is a reasonable value for our current setup and in agreement with other measurements of ours [13].

In conclusion, we have studied three-body recombination involving a single trapped ion and two of its parent atoms at collision energies approaching the sub-mK regime. With a relatively simple model we can understand the two- and three-body collision dynamics and extract corresponding rate coefficients. We observe an increase of the three-body rate coefficient with decreasing collision energy, a behavior that can be expected to become crucial for future experiments targeting even lower temperatures. After a three-body event, ion energies on the order of 0.4 eV were measured, indicating that deeply bound molecules have been created. Since we have not observed Rb_2^+ ions, the formation of Rb_2 seems probable. The ion would then act as an atomic size catalyzer at mK temperatures.

The authors would like to thank Kilian Singer, Piet Schmidt, David Hume, Olivier Dulieu, and Brett Esry for helpful discussions and information. This work was supported by the German Research Foundation DFG within the SFB/TRR21.

[1] H. F. Hess, D. A. Bell, G. P. Kochanski, R. W. Cline, D. Kleppner, and T. J. Greytak, Phys. Rev. Lett. **51**, 483 (1983).

[2] B. D. Esry, C. H. Greene, and J. P. Burke, Phys. Rev. Lett. **83**, 1751 (1999).

[3] E. A. Burt, R. W. Ghrist, C J. Myatt, M. J. Holland, E. A. Cornell, and C. E. Wieman, Phys. Rev. Lett. **79**, 337 (1997).
[4] N. Spethmann *et al.*, arXiv:1204.6051v1.
[5] R. Côté and A. Dalgarno, Phys. Rev. A **62**, 012709 (2000).
[6] A. T. Grier, M. Cetina, F. Oručević, and V. Vuletić, Phys. Rev. Lett. **102**, 223201 (2009).
[7] C. Zipkes, S. Palzer, C. Sias, and M. Köhl, Nature (London) **464**, 388 (2010).
[8] S. Schmid, A. Härter, and J. Hecker Denschlag, Phys. Rev. Lett. **105**, 133202 (2010).
[9] K. Ravi *et al.*, arXiv:1112.5825v1.
[10] F. H. J. Hall, M. Aymar, N. Bouloufa-Maafa, O. Dulieu, and S. Willitsch, Phys. Rev. Lett. **107**, 243202 (2011).
[11] W. G. Rellergert, S. T. Sullivan, S. Kotochigova, A. Petrov, K. Chen, S. J. Schowalter, and E. R. Hudson, Phys. Rev. Lett. **107**, 243201 (2011).
[12] S. Schmid, A. Härter, A. Frisch, S. Hoinka, and J. Hecker Denschlag, Rev. Sci. Instrum. **83**, 053108 (2012).
[13] A. Härter *et al.* (to be published).
[14] D. J. Berkeland, J. D. Miller, J. C. Bergquist, W. M. Itano, and D. J. Wineland, J. Appl. Phys. **83**, 5025 (1998).
[15] R. G. DeVoe, Phys. Rev. Lett. **102**, 063001 (2009).
[16] C. Zipkes, L. Ratschbacher, C. Sias, and M. Köhl, New J. Phys. **13**, 053020 (2011).
[17] M. Cetina, A. Grier, and V. Vuletić, arXiv:1205.2806v1.
[18] Due to the nonthermal energy distribution of the immersed ion, [15,16] we use the median as an energy measure.
[19] See Supplemental Material at http://link.aps.org/supplemental/10.1103/PhysRevLett.109.123201 for (1) description of the fitting routine to acquire $P_{\text{three-body}}$, (2) description of the Monte Carlo simulation, and (3) simulation results assuming purely two-body interactions.
[20] The initial cooldown time is accounted for by adjusting the starting time for each data set.
[21] We deliberately apply an offset electric field of about 6 V/m to increase the excess micromotion energy. In this way, we make three-body reactions unlikely and induce a rapid loss of atoms through binary atom-ion collisions.
[22] K. Singer, U. Poschinger, M. Murphy, P. Ivanov, F. Ziesel, T. Calarco, and F. Schmidt-Kaler, Rev. Mod. Phys. **82**, 2609 (2010).